Fermi National Accelerator Laboratory

FERMILAB-Conf-88/72

The Fermilab Collider D0 Low β System*

A. D. McInturff, J. Carson, T. Collins, K. Koepke,
E. Malamud, P. Mantsch, R. Niemann, and A. Riddiford
Fermi National Accelerator Laboratory
P.O. Box 500, Batavia, Illinois 60510

June 1988

*Presented at the European Particle Accelerator Conference, Rome, Italy, June 7-11, 1988.

THE FERMILAB COLLIDER DØ LOW β SYSTEM

A.D. McInturff, J. Carson, T. Collins, K. Koepke
E. Malamud, P. Mantsch, R. Niemann, A. Riddiford

Fermi National Accelerator Laboratory*
P.O. Box 500
Batavia, Illinois 60510

Abstract

A new low β system has been designed to serve the detector facility under construction at the DØ location of the Fermilab Superconducting Collider. The low β system consists of 18 special cold iron quadrupoles powered as 11 independent circuits that can adjust the β value at the interaction point down to 25 cm. Low beta is achieved with a set of 1.4 T/cm, two shell, high current quadrupoles. Smaller 0.7 T/cm, single shell trim quadrupoles are used to match the low beta insertion to the rest of the accelerator lattice. Gaps have been left in the lattice for electrostatic separators to separate the proton and antiproton beams everywhere except at the desired collision points.

Introduction

The addition of a new colliding beam facility at the DØ long straight section of the Fermilab Tevatron has produced the need for a low beta insertion at this location. A measure of the efficiency of a colliding beam region for physics is the luminosity at its collision point. The luminosity for head-on collisions is given by:

$$L = N_p N_{\bar{p}} B f^o / 4\pi\sigma^2$$

where N_p, and at the Fermilab Collider $N_{\bar{p}}$, are the proton and antiproton bunch intensities, B is the number of bunches in each beam, f^o is the revolution frequency (47 kHz) and σ is the standard deviation of the transverse beam distributions. The formula assumes round, equal sized beams and is not corrected for the variation of beam size through the interaction region. Insofar as σ is proportional to the square root of β, the luminosity is inversely proportional to β^*, the value of the vertical and horisontal β functions at the interaction point. A low beta insertion increases the luminosity by reducing β^* to the lowest practical value.

Recent advances in NbTi metallurgy have resulted in significant gains in the critical current density (1,2) of superconducting cable operating in the 5 T to 8 T magnetic field range and have simplified the design of stronger quadrupoles. The 1.4 T/cm quadrupoles utilized in the DØ low beta insertion have approximately the same aperture but are 40% stronger than the magnets in use at the Tevatron BØ colliding beam location (3,4,5). These higher gradient quadrupoles permit a low beta insertion design for DØ that can be programmed down to a β^* value of 25 cm, a fourfold reduction in β^* relative to the existing BØ β^* design value.

Lattice

The DØ low beta insertion is completely matched to the arcs of the accelerator in betatron and momentum-space. In principle, as many of these insertions can be added to the accelerator as there are free straight sections and each insertion can independently be adjusted through a β^* range of 0.25 m to 1.7 m. Each added insertion raises the tune of the accelerator approximately a half integer unless independent tune correctors are present. The presence of low beta insertions at BØ and DØ will raise the Tevatron tunes to 20.58 and 20.59.

The currently operating BØ low beta system produces a large horizontal dispersion wave and is scheduled to be replaced with an insertion similar to the DØ design. Should budget or other constraints prevent a simultaneous installation at BØ and DØ, an interim geometry which augments the present BØ insertion with DØ low beta spools will be implemented. A lattice solution for operating the Tevatron in this "mixed mode" exists.

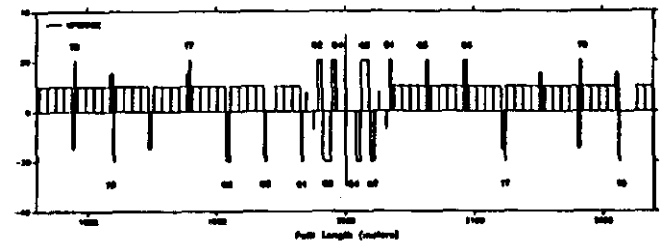

Figure 1. Elements of the Low Beta Lattice

The geometry of the new low beta insertion is shown in Figure 1. Each insertion is composed of 18 independently powered quadrupoles that are physically placed approximately symmetric around the straight section and have magnetic gradients roughly antisymmetric relative to the center of the straight section. A field free region 15.24 m long, equal to the free region at the existing BØ straight section, remains for the detector. Two 9 m long regions located between Q1 and Q2 on both sides of the interaction region are reserved for the future installation of electrostatic separators.

Quadrupoles Q1 through Q5 are separate 1.4 T/cm magnets; the Q6 quadrupoles are 1.4 T/cm magnets physically joined to a "spool" piece. Spool pieces are located around the ring next to each accelerator lattice quadrupole. Dependent on their lattice location, they contain field correction magnets,

Table 1. Magnet Lengths, Fields, Currents

Magnet Number	Magnetic Length (cm)	Maximum Gradient (T/cm)	Maximum Current (A)
Q1	137.34	.5858	2011
Q2	335.28	1.4013	4811
Q3	589.28	1.3824	4746
Q4	335.28	1.4013	4811
Q5	137.34	.8217	2821
Q6	60.64	1.4070	4832
T7	54.61	.6328	1086
T8	54.61	.1441	247
T9	54.61	.5634	967

*Operated by Universities Research Association, Inc.,under contract with the U.S. Department of Energy.

cryogenic and quench protection equipment and all other required functions not readily implemented in the normal lattice magnets. Quadrupoles T7 through T9 are 0.7 T/cm magnets that replace unused correction magnets in existing spools. Most of the 1.4 T/cm magnets are powered as pairs with 5 kA buses that cross the straight section. The Q2 and Q4 magnets have equal currents and are powered on a common 5 kA circuit. Each 0.7 T/cm magnet has its own 1.5 kA circuit. Additional magnet data are given in Table 1.

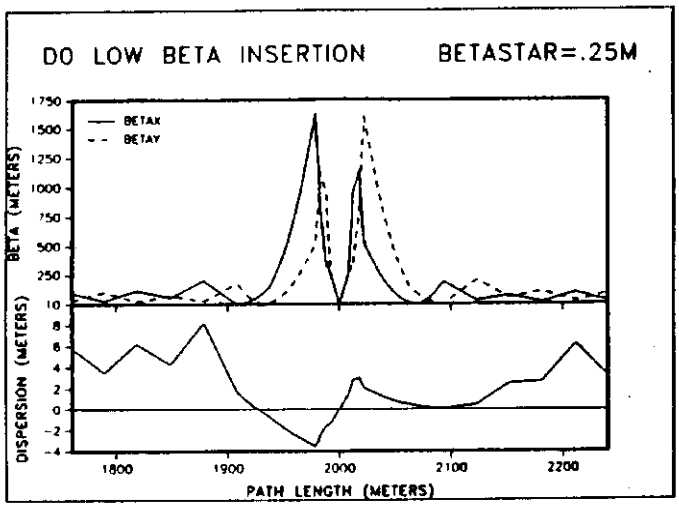

Figure 2. Beta and Horizontal Dispersion for β^*=25 cm

Figure 2. shows the beta functions and horizontal dispersion of the low beta insertion for a β^* value of 25 cm. The β functions follow the symmetry of the low beta quadrupoles and are approximately antisymmetric around the center of the insertion. The peaks in the β functions (1600 m), the bore tube and unavoidable field errors in the low beta quadrupoles combine to set the lower β^* limit for the lattice. The lack of symmetry in dipole placement explains the lack of symmetry of the horizontal dispersion through the straight section. The horizontal dispersion is zero at the interaction point. The vertical dispersion is approximately zero throughout the ring.

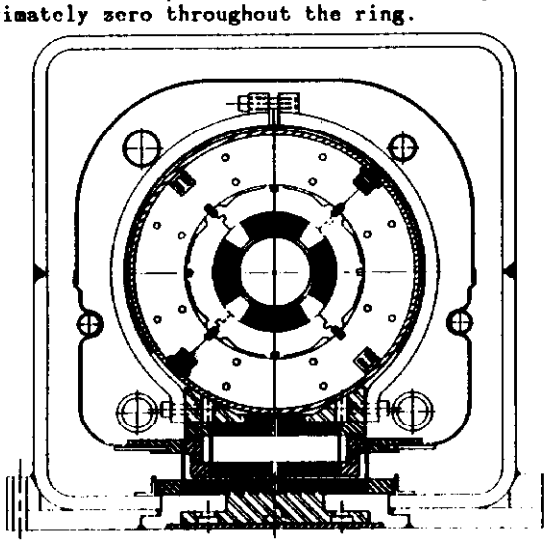

Figure 3. Cross-section of the 2-shell Quadrupole

2-shell Quadrupole

A cross-section of the 1.4 T/cm low beta quadrupole is shown in Figure 3. The quadrupole is a cold iron, 2-shell superconducting magnet with a cryostat based on the design of the SSC dipole (6). The magnet's bore tube and coil inner diameters are 6.858 cm and 7.62 cm respectively. The coils are rigidly clamped with aluminum collars which in turn are clamped by the 17.0 cm inner diameter, 26.7 cm outer diameter magnetic yoke. Channels located at 4-fold symmetric low field regions of the yoke are used to align in azimuth the collared coil to the yoke or contain high current buses and instrumentation leads. A zero clearance stainless steel shell surrounds the yoke and is longitudinally seam-welded to produce a rigid "cold mass". The cold mass is surrounded by a 2-phase helium channel, a liquid nitrogen temperature shield and a thick-walled vacuum vessel. Shorter versions of the SSC style post support the cold mass and heat shields within the steel vacuum vessel. The outer dimension of the 45.72 cm square vacuum vessel was chosen to fit the limited clearance present in the BØ detector.

The isothermal surfaces of the cryostat are separated by vacuum and layers of superinsulation, and contain two LN and two helium tubes. The additional cryogenic tubes in the low beta cryostats allows the cryogenic end box normally located at the end of a magnet string to be placed between magnets Q1 and Q2, thereby clearing the region of the magnet closest to the interaction point for detector components. The total estimated heat leak of the low beta insertion is 52 W. Existing refrigerators (4.6 K - 4.8 K) cool the low beta magnets since they are cryogenically coupled to the accelerator magnets on either side of the straight section.

The quadrupoles are wound with 36 strand Rutherford type superconducting cable. Each pole contains 19 inner and 28 outer turns. The 0.528 mm diameter strands contain 612 filaments, 13 microns in diameter and a copper to superconducting ratio of 1.5:1. It is anticipated that the NbTi can reach a current density in excess of 3000 A/mm at 4.2 K and 5T. The magnet load line is show in Figure 4. The transfer function for the magnet is 0.291 T/cm/kA.

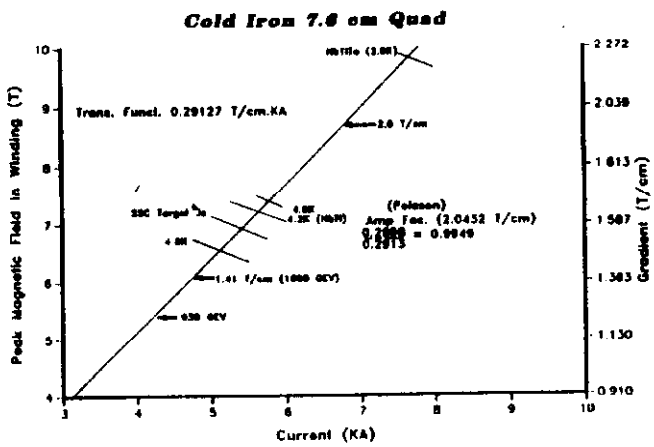

Figure 4. 2-shell Quadrupole Magnet Load Line

The expected body quadrupole field has been calculated using the MAGFLD and POISSON computer codes. The results of the calculation are shown in Table 2. The normalised field errors (NFE), the higher harmonic field strength divided by the quadrupole field strength, are evaluated at a point 2.54 cm off axis in units of 10^{-4} and n=6 represents the 12-pole, n=10 the 20-pole, etc. The actual magnet field will also depend on construction errors which can introduce other normal and skew harmonics,

principally a sextupole component. Copper wedges have been added to the inner and outer coils to reduce the 12-pole and 20-pole of the two-dimensional field of the magnet. These field terms have also been minimized at the magnet ends with turn spacers and by adjusting the relative length of the inner and outer coils. Iron saturation is expected to lower the quadrupole transfer function by .51% from linear at 1.4 T/cm.

Table 2. Calculated Field Errors

n	6	10	14	18	22	26	30
NFE	0.46	-0.15	1.20	-0.53	0.0014	0.012	-0.0007

The large filament diameter of the 1-shell and 2-shell low beta quadrupoles will degrade the ramp rate behavior of these magnets. This is not a problem during colliding beam operation as the ramp rate of the infrequent acceleration period can be adjusted to the capabilities of these magnets. During fixed target operation, all the 1-shell and the Q6 2-shell magnets are not energized; the low beta magnets within the DØ straight section are replaced with the original components used for beam extraction; and the BØ low beta insertion is reprogrammed to approximate a "normal beta" straight section. The required field range of the 2-shell low beta magnets during fixed target operation is less than half their maximum gradient.

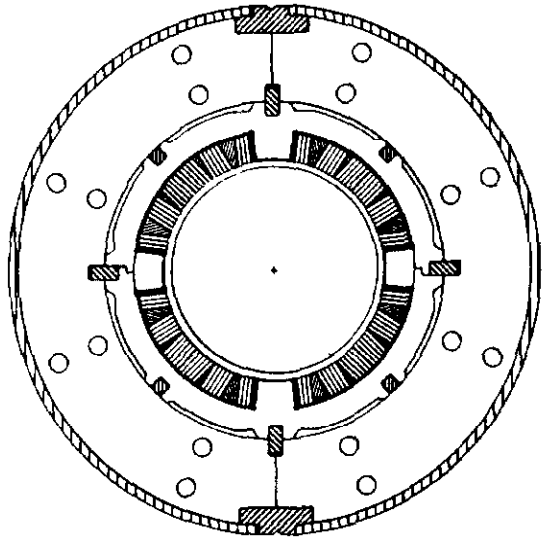

Figure 5. Cross-section of the 1-shell Quadrupole

1-shell Quadrupole

The cross-section of the 1-shell quadrupole cold mass is shown in Figure 5. This magnet replaces unused correction magnets in existing spools and therefore does not require a new cryostat design. The bore tube and coil inner diameters are identical to the 2-shell design. The magnet cold mass has an outer diameter of 19.05 cm, a physical length including end connections of 76.2 cm and an effective field length of 54.61 cm. The load line for this magnet is shown in Figure 6. The magnet transfer function is .5825 T/cm per kA. The magnet needs to operate at a peak gradient of 0.7 T/cm.

In order to reduce the operating current and the heat load from power leads, this magnet is wound with 5-in-1 cable. Each pole has 13 turns and each turn contains 5 insulated monolithic conductors for an effective 65 turns per pole. The monolithic conductors (1.09 mm x 1.76 mm without insulation) are manufactured from the same material as used in the 2-shell magnets. The monolithic conductors contain 612 filaments, each 20 μm in diameter and have a copper to superconductor ratio of 1.5:1.

The calculated field errors (body plus ends) for this magnet are listed in Table 3. As in the 2-shell quadrupole, shims have been used in the coil and end turns to minimize the 12-pole and 20-pole terms.

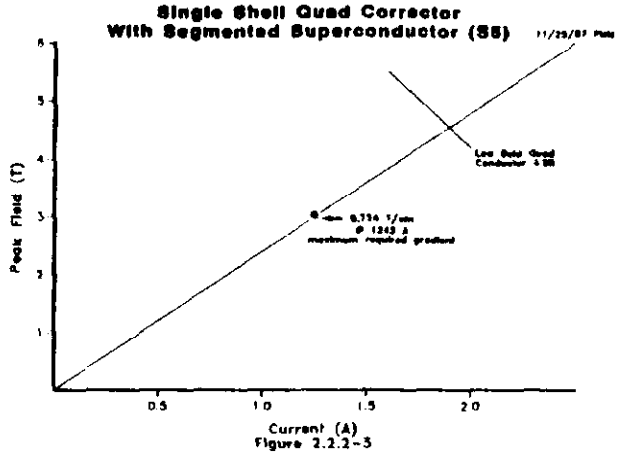

Figure 6. 1-shell Quadrupole Magnet Load Line

Table 3. Calculated Field Errors

n	6	10	14	18	22	26
NFE	0.0	0.0	0.8	-0.14	0.11	-.004

Project Status

Sample cable has passed the required mechanical and electrical specifications. Cable in quantity is scheduled to arrive within a month. The tooling to wind, press, cure and collar the 2-shell quadrupoles has been assembled and tested with old superconducting cable. The 1-shell coils will be wound with the inner coil 2-shell tooling. Coil sections to verify coil placement, insulation suitability, preload and component tolerances have been successfully completed. A 1 m test magnet has been fabricated and is undergoing tests in a vertical dewar to primarily confirm field quality, heat load during ramping and quench protection schemes.

REFERENCES

1. D. Larbalestier, et al., Cryogenics, Vol. 27, 171,(1987)
2. P. Lee and D. Larbalestier, Act. Metal. ,Vol. 35, 2523,(1987)
3. D. Johnson,IEEE Trans. on N.S.,NS-32,1672,(1985)
4. K. Koepke, E. Fisk, G. Mulholland, H. Pfeffer, IEEE Trans. on N.S.,NS-32,1675,(1985)
5. D. Finley, R. Johnson and F. Willeke, IEE Trans. on N.S.,NS-32,1678,(1985)
6. R. Niemann, et al., Adv. Cryo. Engr.,Vol.31, 37,(1985)